Near threshold rotational excitation of molecular ions by electron-impact

A Faure[1], V Kokoouline[2], Chris H Greene[3] and Jonathan Tennyson[4]

[1] Laboratoire d'Astrophysique, UMR 5571 CNRS, Université Joseph-Fourier, B.P. 53, 38041 Grenoble cedex 09, France

[2] Department of Physics, University of Central Florida, Orlando, Florida 32816, USA

[3] Department of Physics and JILA, University of Colorado, Boulder, Colorado 80309-0440, USA

[4] Department of Physics and Astronomy, University College London, Gower Street, London WC1E 6BT, UK

E-mail: `afaure@obs.ujf-grenoble.fr`

Abstract.

New cross sections for the rotational excitation of H_3^+ by electrons are calculated *ab initio* at low impact energies. The validity of the adiabatic-nuclei-rotation (ANR) approximation, combined with R-matrix wavefunctions, is assessed by comparison with rovibrational quantum defect theory calculations based on the treatment of Kokoouline and Greene (*Phys. Rev. A* **68** 012703 2003). Pure ANR excitation cross sections are shown to be accurate down to threshold, except in the presence of large oscillating Rydberg resonances. These resonances occur for transitions with $\Delta J = 1$ and are caused by closed channel effects. A simple analytic formula is derived for averaging the rotational probabilities over such resonances in a 3-channel problem. In accord with the Wigner law for an attractive Coulomb field, rotational excitation cross sections are shown to be large and finite at threshold, with a significant but moderate contribution from closed channels.

PACS numbers:

1. Introduction

Rotational excitation of positive molecular ions is a major mechanism by which slow electrons lose energy in partially ionized molecular gas. The efficiency of this process is a significant parameter in various applications, for example the interpretation of dissociative recombination experiments (Lammich *et al* 2003, Kokoouline and Greene 2003) or the determination of the density and temperature conditions in the diffuse interstellar medium (Lim *et al* 1999, Faure *et al* 2006). A good knowledge of rotational (de)excitation cross sections is therefore required for a variety of molecular ions and over a wide range of collisional energies and rotational levels. In contrast to neutral molecules, however, little attention has been given to the electron-impact

excitation of molecular ions. These are indeed more difficult to study experimentally and only a few theoretical treatments have been reported so far. The reference method for computing electron-impact excitation cross sections has been the Coulomb-Born (CB) approximation (Cho and Dalgarno 1974, Cho 1975, Dickinson and Muñoz 1977, Neufeld and Dalgarno 1989). This approach assumes that the collisional cross sections are entirely dominated by long-range interactions. The CB theory thus predicts that transitions with ΔJ=1 and 2 only are allowed for dipole and quadrupole interactions, respectively. Recent *ab initio* R-matrix studies on several astronomically important molecular ions have shown, however, that this prediction is incorrect and that the inclusion of short-range interactions is crucial, particularly for ions with small (or zero) dipole or transitions with $\Delta J > 1$ (see Rabadán *et al* (1998), Faure and Tennyson (2002b) and references therein).

These R-matrix studies were, however, hampered by the use of the adiabatic-nuclei-rotation (ANR) approximation. The ANR theory is expected to become invalid close to a rotational threshold because it neglects the rotational Hamiltonian (see, e.g., Lane (1980)). This leads to an ambiguous interpretation of the ANR energy because the electron energy in the exit channel of a near-threshold inelastic collision is very small while the assumption of rotational degeneracy sets this energy equal to that of the entrance channel. As a result, if the ANR energy is interpreted (as usual) as the initial kinetic energy, then excitation cross sections are non-zero at and below threshold. In previous R-matrix works, this artefact was corrected by multiplying the ANR cross sections by the kinematic ratio k'/k, where k (k') is the initial (final) momentum of the electron. This simple method, which forces the cross sections to zero at threshold, is widely used in the case of neutral molecules (Morrison 1988). The resulting cross sections, however, do not obey the proper threshold law, when the molecular target has a nonzero charge. In the present work, near threshold rotational excitation of H_3^+ by electron-impact is investigated by comparing ANR cross sections with independent calculations based on the quantum defect theory and rotational-frame-transformation (MQDT-RFT) approach (Fano 1970, Chang and Fano 1972, Child and Jungen 1990, Kokoouline and Greene 2003) To our knowledge, this is the first quantitative assessment of the validity of the adiabatic approximation for electron-impact rotational excitation of a charged target molecule. The theoretical treatments are introduced in the next section. Comparisons of cross sections obtained at different levels of theory are presented in section 3. Conclusions are summarized in section 4.

2. Theory

We consider the following process between an electron and a symmetric-top molecular ion:

$$e^-(E_k) + ION(JKM) \rightarrow e^-(E'_k) + ION(J'K'M'), \quad (1)$$

where J is the ionic rotational angular momentum, K and M its projections along the body-fixed (BF) and the space-fixed (SF) axes, respectively, and E_k (E'_k) is the initial

(final) kinetic energy of the electron. The relation between E_k and E'_k is:

$$E'_k = E_k + (E_{JK} - E_{J'K'}), \tag{2}$$

where the energy of the state (JK) is given in the rigid rotor approximation by:

$$E_{JK} = BJ(J+1) + (A-B)K^2, \tag{3}$$

with A and B being the rotational constants. It should be noted that vibrational energy splittings of H_3^+ are much larger than rotational splittings, with the first excited vibrational level $\{01^1\}$ being 0.3 eV above the ground vibrational level $\{00^0\}$. In the following, we will assume that the initial and final vibrational state of the ion is $\{00^0\}$ and that the incident electron energy is less than 0.3 eV.

2.1. ANR method

We follow the implementation of the ANR theory for symmetric-top molecular ions as presented in Faure and Tennyson (2002b). The key quantities in this approach are the T-matrix elements which are produced in the BF frame of reference and are then transformed through the conversion of the BF asymptotic scattering amplitude to the SF frame. In this approach, the rotational Hamiltonian is neglected and there is an ambiguity in defining the BF asymptotic electron energy, E_{bf}, which can be taken equal to the kinetic energy in the entrance (E_k) or exit (E'_k) channels, or even to some other values (see Morrison (1988) and references for neutral targets therein). The usual choice, however, is to take E_{bf} as the initial kinetic energy, E_k. The integral ANR rotationally inelastic cross section for a symmetric-top molecule is then given by (Faure and Tennyson 2002b):

$$\sigma^{\rm ANR}_{JK\to J'K'}(E_k) = \frac{(2J'+1)\pi}{2E_k} \sum_{jm_j} (2j+1) \times \begin{pmatrix} J & J' & j \\ K & -K' & m_j \end{pmatrix}^2 \sum_{ll'} |M^{jm_j}_{ll'}(E_k)|^2 \tag{4}$$

with

$$M^{jm_j}_{ll'}(E_k) = \sum_{mm'hh'p\mu} \bar{b}^{p\mu}_{lhm} \begin{pmatrix} l & l' & j \\ -m & m' & m_j \end{pmatrix} \bar{b}^{p\mu}_{l'h'm'} T^{p\mu}_{lh,l'h'}(E_k) \tag{5}$$

where l (l') is the initial (final) electron orbital momentum, $T^{p\mu}_{lh,l'h'}$ are the BF T-matrix elements belonging to the μth component of the pth irreducible representation (IR) of the molecular point group, with h distinguishing between different elements with the same ($p\mu l$). The $\bar{b}$ coefficients are discussed, for example, in Gianturco and Jain (1986). The T-matrix is as usually defined in terms of S-matrix as

$$\boldsymbol{T} = \mathbf{1} - \mathbf{S} \tag{6}$$

and the cross section can be expressed in terms of the SF S-matrix by the familiar formula:

$$\sigma^{\rm ANR}_{JK\to J'K'}(E_k) = \frac{\pi}{2E_k(2J+1)} \sum_{J_{\rm tot}ll'} (2J_{\rm tot}+1)|\delta_{JJ'}\delta_{KK'}\delta_{ll'} - S^{J_{\rm tot}}_{JKl,J'K'l'}(E_k)|^2, \tag{7}$$

where $\boldsymbol{J}_{\rm tot} = \boldsymbol{J} + \boldsymbol{l}$ is the total angular momentum. It should be noted that the ambiguous choice $E_{bf} = E_k$ leads to excitation cross section that are non-zero below threshold. A common method for forcing the cross sections to zero at threshold is to multiply these by the ratio of the final and initial momentum of the electron, k'/k (Morrison 1988). This was used in particular in previous R-matrix works (Faure and Tennyson 2002b). However, the ANR T-matrix elements still do not exhibit the proper dependence on k' in this limit, for an ionic target. Alternatives such as $E_{bf} = E'_k$ are possible but still should not give the correct threshold laws for the T-matrix elements. Furthermore, the principle of detailed balance is not rigorously satisfied near threshold. This will be further discussed in section 2.3.

The e^-+H_3^+ BF T-matrices were taken from the R-matrix calculations of Faure and Tennyson (2002a). The geometry of the ion was frozen at its equilibrium position corresponding to an equilateral triangle with D_{3h} symmetry. The e^-+H_3^+ scattering model was constructed using the four lowest target electronic states and the continuum orbitals were represented using the GTO basis set given by Faure *et al* (2002) which include all angular momentum up to $l_{\rm max} = 4$ and is optimized to span energies below 5 Ryd. As discussed in Faure and Tennyson (2002b), rotationally inelastic cross sections were found to be entirely dominated by low partial waves, with more than 90 % arising from $l = 1$, and ANR cross sections were obviously unaltered by augmenting them with quadrupolar CB calculations for partial waves with $l > 4$. Collisional selection rules are detailed in Faure and Tennyson (2002b).

2.2. MQDT-RFT method

We follow the implementation of the MQDT-RFT theory as presented by Kokoouline and Greene (2003, 2004). The e^-+H_3^+ scattering model is based on *ab initio* H_3^+ and H_3 potentials independent from the R-matrix model presented above. In this framework, originally developed for the dissociative recombination of H_3^+, first, one constructs the energy-independent S^{BF}-matrix in a basis better adapted for BF (see Kokoouline and Greene (2003, 2004) and references therein). The S^{BF}-matrix depends on the three internuclear coordinates $\mathcal{Q}$ and the projection Λ of the electronic orbital momentum on the molecular axis. Thus, we define the elements of the scattering matrix as

$$\langle \mathcal{Q};\Lambda|\hat{S}|\mathcal{Q}';\Lambda'\rangle = S^{BF}_{\Lambda;\Lambda'}(\mathcal{Q})\delta(\mathcal{Q},\mathcal{Q}'). \tag{8}$$

The S^{BF}-matrix in this representation is diagonal with respect to the rotational quantum numbers $J_{\rm tot}$, $K_{\rm tot}$ and $M_{\rm tot}$ of the whole molecule and the continuous coordinate $\mathcal{Q}$. To completely define basis functions $|b\rangle$ in the BF, in addition to Λ and $\mathcal{Q}$, the rotational quantum numbers $J_{\rm tot}$, $K_{\rm tot}$ and $M_{\rm tot}$ must be also specified; for brevity they are omitted in the above equation. For the matrix element $S^{BF}_{\Lambda;\Lambda'}(\mathcal{Q})$ we will also use the notation $\langle b|\hat{S}|b'\rangle$. The next step in the MQDT-RFT is to obtain the S-matrix in the basis $|s\rangle$ corresponding to the laboratory or SF coordinate system. In this basis, the good quantum numbers are the vibrational quantum numbers (for example, $\{v_1, v_2^{l_2}\}$, if the normal mode approximation is used) and rotational quantum numbers $J_{\rm tot}, J, K, M, l, m$

defined above. In the following, we will not specify any other conserved quantum numbers that are the same in the both bases, such as the total nuclear spin and the irreducible representation of the total wavefunction. The SF S-matrix is determined by carrying out a unitary transformation from the BF basis to the SF basis:

$$S_{s;s'} = \sum_{b,b'} \langle s|b\rangle \langle b|\hat{S}|b'\rangle \langle b'|s'\rangle\,, \tag{9}$$

where the summation indicates a sum over discrete indices and an integration over the continuous coordinates $\mathcal{Q}$. The explicit form of the the unitary transformation matrix elements $\langle s|b\rangle$ is given in Eq.(27) of Kokoouline and Greene (2004).

The transformation of Eq. 9 is truly unitary only if the vibrational basis in the SF representation is complete. In calculations, one always adopts a finite vibrational basis set that is not complete. It should be sufficiently large to represent properly the vibrational states contributing to the process of interest. In practice the vibrational basis set is calculated within a finite volume, and one can impose outgoing-wave (Siegert) boundary conditions at its surface to account for the fact that some of the incident electron flux can be diverted through the collision into dissociative channels, as in Hamilton and Greene (2002) and Kokoouline and Greene (2003). The procedure of transformation from the BF to SF representations described above is called the rovibrational frame transformation in MQDT. It accounts for the coupling between electronic, rotational and vibrational motion of the molecule. In contrast to the MQDT-RFT approach, the rotational dynamics of the system is not included in the ANR.

The unitary transformation of the S-matrix from the body frame to the laboratory frame, as described in the preceding paragraph, is similar in spirit to that described by Chase (1956,1957). But one important physical difference is that, whereas the Chase approximation was intended to be applied only in energetically open collision channels, in the MQDT-RFT the transformed scattering matrix S includes (weakly) closed channels as well. When the incident electron collides with a singly-charged molecular ion of size r_0, its kinetic energy is increased by $1/r_0$, and consequently scattering into weakly-closed channels is often an important class of pathways, even for entrance or exit scattering processes that occur right at threshold with zero asymptotic kinetic energy. Every such threshold has an infinite number of Rydberg levels converging to it. For this reason, the transformed S does not yet represent the physical scattering matrix (Aymar *et al* 1996). In fact, it represents the actual scattering matrix S^{phys} only in energy ranges where *all* of the channels $|s\rangle$ are open for electron escape, i.e. where the total energy of the system is higher than the energy of the highest relevant ionization channel $|s\rangle$ threshold. When at least one channel is closed, the physical scattering matrix S^{phys} is obtained from S using the standard MQDT channel-elimination formula (see Eq. (2.50) in Aymar *et al* (1996) or Eq. (38) in Kokoouline and Greene (2004)).

In the H_3^+ DR studies carried out by Kokoouline and Greene (2003, 2004), the treatment has been limited to the dominant p-wave component (l=1) of the incident electron wavefunction because the p-wave has the largest contribution into the DR cross-section. This partial wave also has the largest effect on the rotational excitation

probabilities considered in the present study. When all channels $|s\rangle$ are open for electron escape, the scattering matrix is energy-independent. (This is within the frequently-adopted approximation of energy-independent quantum defects, which can be improved upon when necessary, as has been discussed, e.g., by Gao and Greene (1990).) When there are closed channels that are coupled to open channels, the autoionizing Rydberg series associated with the closed ionic channels introduce a strong energy dependence into the physical scattering matrix. Consequently, the resulting cross-sections reflect these autoionizing resonance features that are strongly dependent on the energy. Examples of such energy dependences that arise in electron collisions with H_3^+ are demonstrated below. These rotational autoionizing resonances have been thoroughly studied in both experimental (Bordas *et al* (1991)) and theoretical (Stephens and Greene (1995), Kokoouline and Greene (2004)) studies of H_3 photoabsorption processes.

MQDT-RFT calculations including the complete rovibrational frame transformation and the Jahn-Teller effect have shown that the probability of rotational excitation $|\boldsymbol{S}^2|$ is weakly energy-dependent in the region between the $\{00^0\}$ and $\{01^1\}$ vibrational levels (Kokoouline and Greene 2003). The Rydberg resonances present in the rotational-excitation spectrum have in general small widths. However, for transitions involving symmetries with more than two rotational channels, the rotationally inelastic probabilities are actually nearly energy-independent only at electron energies above the highest channel (all coupled rotational levels are open). For a 3-channel problem, there are thus an infinite number of purely rotational Rydberg resonances at electron energies between the second and third channel thresholds. This is illustrated in Fig. 1 for the transition (1, 1)→(2, 1) at $J_{\rm tot} = 2$ (there is no p-wave Rydberg series attached to (3, 1) at $J_{\rm tot} = 1$). Note that for the reverse process (2, 1)→ (1, 1), all curves in Fig. 1 would be simply shifted towards zero electron-impact energy, in accordance with the detailed balance principle (see section 2.3).

It can be seen in Fig. 1 that the pure MQDT-RFT calculation (bottom panel) is in very good agreement with the much more expensive rovibrational MQDT treatment (top and middle panels). In the top panel, we observe the complicated structure introduced by the inclusion of the vibrational motion at energies above the (3, 1) threshold. In this energy range, there are many narrow resonances corresponding to vibrationally excited states of bound H_3 Rydberg states. If one considers the integral over the resonance region, however, these resonances do not change the probability significantly. Thus, as previously observed by Rabadán *et al* (1998) for diatomic ions, a detailed treatment of vibrational motion is unnecessary to obtain reliable thermally-averaged rotational excitation rate coefficients of the type normally needed in astrophysical applications. On the other hand, in the region between the (2, 1) and (3, 1) channels, Rydberg resonances are found to increase the rotational probability by about a factor of 2 on average, i.e., the value of 0.15 just above the (3, 1) channel increases discontinuously to an averaged value of 0.29. Note that higher closed channels involving partial waves with $l > 1$ are negligible. Physically it means that incident electrons in partial waves with $l > 1$, for the energy range considered here, can not approach the ion closely enough to

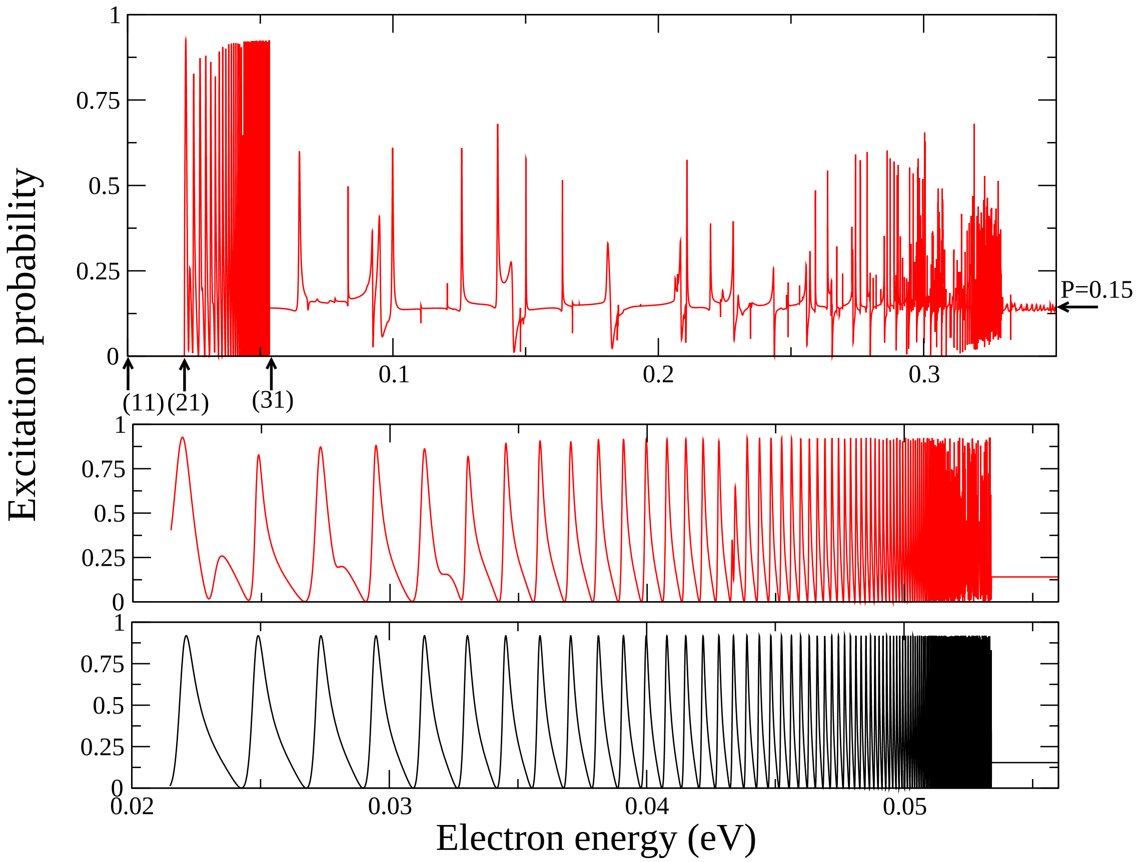

Figure 1. Inelastic rotational excitation probability from the $(1, 1)$ state of H_3^+ to the $(2, 1)$ state as a function of electron-impact energy. The probability is approximately energy-independent at the value 0.15 just above the $(1, 1)\rightarrow(3,1)$ rotational threshold. A pure MQDT-RFT calculation is presented at the bottom, while the upper two frames demonstrate the prediction from a fuller MQDT calculation that includes rovibrational autoionizing states associated with higher closed channel thresholds. The arrows below the upper panel indicates energies of the (1,1), (2,1), and (3,1) rotational states of the ion.

be able to excite it. From the MQDT point of view, it means that the quantum defects for molecular states with $l > 1$ are close to zero. Indeed, calculated cross sections for transitions with $\Delta J > 2$ or $\Delta K \neq 0$ are 3 to 4 orders of magnitude smaller than those with $\Delta J = 1, 2$ and $\Delta K = 0$ (Faure and Tennyson 2002b). Resonances due to these low probability transitions do not therefore contribute significantly to the cross section. In the following, we will only consider 2- and 3-channel problems (i.e. transitions with $\Delta J = 1$ and 2) and two possible energy ranges: above and below the highest channel threshold.

2.2.1. Above the highest channel threshold Since we have restricted the frame transformation analysis in this paper to the purely rotational FT, the ionization channels in the energy-independent scattering matrix $S_{s;s'}$ differ only in their rotational quantum

numbers. The vibrational state is the same for all the channels, namely, the ground vibrational state of the ion. Therefore, the integral over the vibrational coordinates $\mathcal{Q}$ in Eq. (9) (or in Eq. (27) of Kokoouline and Greene (2004)) is the same for all the matrix elements $S_{s;s'}$. Although the BF scattering matrix is not diagonal at all geometries in the BF rotational quantum number Λ, the integral over the vibrational coordinates $\mathcal{Q}$ is not zero only when $\Lambda = \Lambda'$. This is because the non-diagonal elements of the BF matrix describe Jahn-Teller physics, which effectively couples only vibrational states belonging to different irreducible representations. Therefore, the integrals over the vibrational coordinates of the ground vibrational state can be viewed as an effective diagonal 3×3 or 2×2 scattering matrix with elements $\mathrm{e}^{2\pi \mathrm{i} \bar{\mu}_\Lambda}$, where $\bar{\mu}_\Lambda$ represent the quantum defects averaged over the vibrational state. They are very close to the H_3 Born-Oppenheimer quantum defects at the minimum of the H_3^+ potential surface. The SF scattering matrix elements become in this approximation (Eq. (43) of Kokoouline and Greene (2003)):

$$S^{(J_{\rm tot},K_{\rm tot},l)}_{J,K;J',K'} = \sum_{\Lambda} (-1)^{K+K'} \sqrt{(2J+1)(2J'+1)} \mathrm{e}^{2\pi \mathrm{i} \bar{\mu}_\Lambda} \times \tag{10}$$

$$\times \begin{pmatrix} l & J_{\rm tot} & J' \\ -\Lambda & K_{\rm tot} & -K' \end{pmatrix} \begin{pmatrix} l & J_{\rm tot} & J \\ -\Lambda & K_{\rm tot} & -K \end{pmatrix}. \tag{11}$$

In all calculations below we have used $\bar{\mu}_0$=0.05 and $\bar{\mu}_{\pm 1}$=0.39 for the p-wave quantum defects, as in Kokoouline and Greene (2003). The above SF scattering matrix is energy independent and describes the electron-ion scattering only for energies above the highest ionization channel. The corresponding rotational probabilities for a set of symmetries and nuclear spins can be found in Table VI of Kokoouline and Greene (2003). Finally, the rotationally inelastic cross section is obtained as:

$$\sigma^{\rm RFT}_{JK\to J'K'}(E_k) = \frac{\pi}{2E_k(2J+1)} \sum_{J_{\rm tot} K_{\rm tot}} (2J_{\rm tot}+1) |\delta_{JJ'}\delta_{KK'} - S^{(J_{\rm tot},K_{\rm tot},l)}_{J,K;J',K'}|^2, \tag{12}$$

2.2.2. Between the 2$^{\rm nd}$ *and 3*$^{\rm rd}$ *channel* The physical scattering matrix S^{phys} appropriate for this energy range is obtained from the matrix of Eq. (12) by the usual MQDT closed-channel elimination procedure (Aymar *et al* 1996). To simplify the formulae we omit here all indexes and superscripts other than 1,2, and 3. If channels 1 and 2 are open and channel 3 is closed the amplitude of the excitation $1 \to 2$ is given by

$$S^{phys}_{2;1}(E) = S_{2;1} - \frac{S_{2;3}S_{3;1}}{S_{3;3} - \mathrm{e}^{-2\mathrm{i}\beta(E)}} \tag{13}$$

$$\text{with}\, \beta(E) = \frac{\pi}{\sqrt{2(E_3 - E)}},$$

where E_3 is the ionization threshold energy of channel 3. The $1 \to 2$ excitation probability is given by $P_{1;2} = |S^{phys}_{2;1}(E)|^2$ and is shown in the lowest panel of Fig. 1. The probability depends strongly on the energy owing to the Rydberg series of resonances

attached to channel 3. We have derived an analytical expression for the excitation probability $\bar{P}_{1;2}$ averaged over energy in this region. Since $P_{1;2}$ is a periodic function of β, we average over just one period $[0, \pi]$, i.e. over just one unit in the effective quantum number of the closed channel 3:

$$\bar{P}_{1;2} = \frac{1}{\pi} \int_0^{\pi} |S_{2;1}^{phys}(E)|^2 d\beta \,. \tag{14}$$

We change this into a contour integral by making the variable change

$$z = \mathrm{e}^{2\mathrm{i}\beta} \,, dz = \mathrm{e}^{2\mathrm{i}\beta} 2\mathrm{i} d\beta \,, \tag{15}$$

and we obtain the following form for $\bar{P}_{1;2}$:

$$\frac{1}{2\pi\mathrm{i}} \oint_{unit\,circle} \frac{dz}{z} \frac{\left[S_{2;1}(S_{3;3} - \frac{1}{z}) - S_{2;3}S_{3;1}\right]\left[S_{2;1}^*(S_{3;3}^* - z) - S_{2;3}^*S_{3;1}^*\right]}{(S_{3;3} - \frac{1}{z})(S_{3;3}^* - z)} \,.$$

This integral has two simple poles $z = 0$ and $z = S_{3;3}^*$ inside the circle. The residue of the integrand at $z = 0$ is

$$\frac{|S_{2;1}|^2 S_{3;3}^* - S_{2;1}S_{3;1}^*S_{2;3}^*}{S_{3;3}^*} \tag{16}$$

and the residue at $z = S_{3;3}^*$ is

$$\frac{S_{3;1}^*S_{2;3}^*\left(|S_{3;3}|^2 S_{2;1} - S_{2;1} - S_{3;1}S_{2;3}S_{3;3}^*\right)}{S_{3;3}^*\left(|S_{3;3}|^2 - 1\right)} \,. \tag{17}$$

Once these are added, we see that the integral in Eq. (16) can be simplified to give the average excitation probability in the energy range of rotational autoionizing states as

$$\bar{P}_{1;2} = |S_{2;1}|^2 + \frac{|S_{3;1}|^2\,|S_{3;2}|^2}{|S_{3;1}|^2 + |S_{3;2}|^2} \,. \tag{18}$$

We can notice that the above formula is consistent with the fact that Rydberg resonances are important when $|S_{1;3}|^2$ is comparable in magnitude with $|S_{1;2}|^2$ and $|S_{2;3}|^2$. Thus, the larger $|S_{1;3}|^2$ is, the larger are the resonances and their average contribution to the total excitation cross section. It should be also noted that the ratio

$$R = \frac{\bar{P}_{1;2}}{|S_{1;2}|^2} \tag{19}$$

is actually independent of the quantum defects and is entirely controlled by Clebsch-Gordan algebra. In the case of the (1, 1)→ (2, 1) transition, R is equal to 15/7, leading to an analytically averaged value of $\bar{P}_{1;2} = 0.33$, to be compared with the numerically-calculated average value of 0.29 (see Fig. 1). The accuracy of the present analytic approach is therefore estimated to be of the order of 10 %.

Finally, we note that the present analytical averaging can of course be applied to any SF S-matrices, in particular ANR S-matrices that would have been converted to the SF frame of reference. In the following, however, the averaging procedure will be implemented for MQDT-RFT probabilities only.

2.3. Detailed balance

The principle of detailed balance, which is the consequence of the invariance of the interaction under time reversal, states that the transition probabilities $|S_{1;2}|^2$ and $|S_{2;1}|^2$ for a certain inelastic process $|1\rangle \rightarrow |2\rangle$ and its reverse $|2\rangle \rightarrow |1\rangle$ are equal *at a given total energy,* $E_{\rm tot}$, defined as:

$$E_{\rm tot} = E_{k,1} + E_1 = E_{k,2} + E_2, \tag{20}$$

where $E_{k,i}$ is the electron kinetic energy and E_i is the target internal energy. Following this definition, cross sections must obey the formula:

$$\sigma_{1\rightarrow 2}(E_{k,1})g_1 E_{k,1} = \sigma_{2\rightarrow 1}(E_{k,2})g_2 E_{k,2}, \tag{21}$$

where g_i is the statistical weight of the state i. At the MQDT-RFT level of theory, detailed balance is rigorously satisfied, even with the above averaging of probabilities over Rydberg resonances. It should be noted, however, that this would not be the case for the averaged formulae presented above, if cross sections or rate coefficients were averaged over resonances instead of probabilities. At the ANR level of theory, the assumption of target-state degeneracy leads to transition probabilities that are equal *at a given kinetic energy.* As a result, ANR cross sections obey the following formula:

$$\sigma^{\rm ANR}_{1\rightarrow 2}(E_k)g_1 = \sigma^{\rm ANR}_{2\rightarrow 1}(E_k)g_2, \tag{22}$$

and Eq. (21) is generally not satisfied at the ANR level. This problem again reflects the ambiguity in defining the BF asymptotic electron energy. In particular, if this energy is taken equal to the entrance electron energy for an excitation process and to the exit electron energy for the reverse deexcitation process, then Eq. (21) is rigorously satisfied at the ANR level. Moreover, when the transition probability is energy independent, as it is at the MQDT-RFT level for energies above the highest channel, then cross sections obey both Eqs. (21) and (22). This will be further discussed in the next section.

3. Results

Rotationally inelastic cross sections are presented in Figs. 2 and 3 for upward rotational transitions in *ortho-* and *para-* H_3^+. In Fig. 2, the rovibrational MQDT result is compared to the MQDT-RFT and ANR calculations for the transition (1, 1)→ (2, 1). Note that the full MQDT-rovibrational and MQDT-RFT results include contributions from $J_{\rm tot} = 1$ and $J_{\rm tot} = 2$. We can first notice that the agreement between MQDT-RFT and ANR cross sections is extremely good above the highest (3, 1) channel, with relative differences of less than 2 %. In this energy range, we also notice in the full MQDT treatment a number of narrow resonances that correspond to vibrationally excited states of bound H_3 Rydberg states, as observed in Fig. 1 for $J_{\rm tot} = 2$. Between the (2, 1) and (3, 1) channels, the ANR cross section is found to significantly underestimate the averaged cross section owing to the appearance of large purely rotational Rydberg resonances. In this energy range, the MQDT-RFT calculation includes the analytical averaging of probabilities

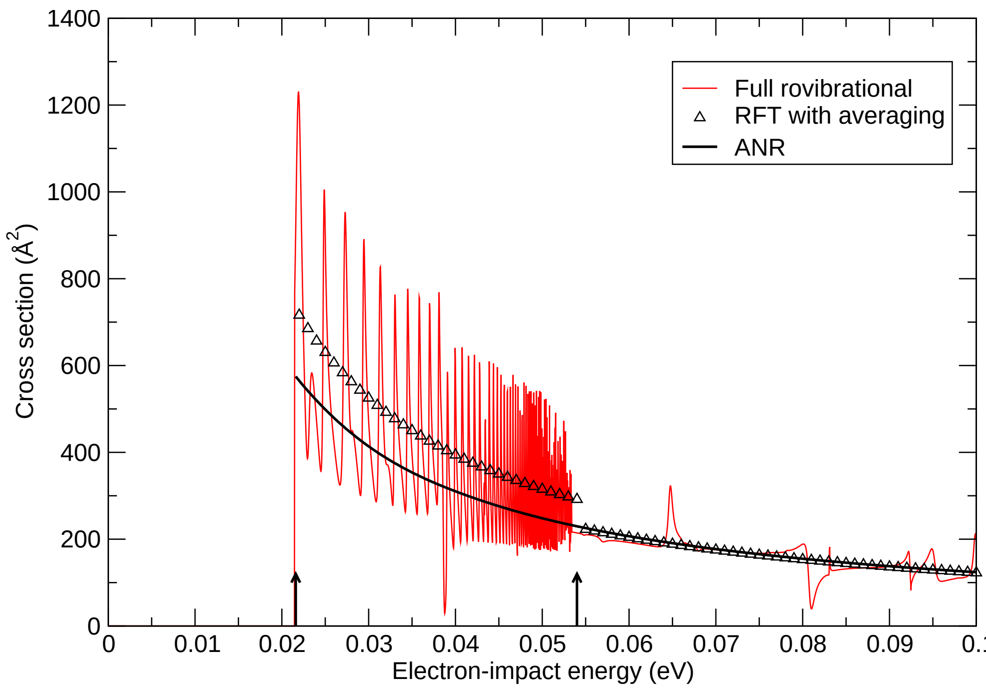

Figure 2. Rotationally inelastic excitation cross sections for the transition (1, 1) → (2, 1) in H_3^+ as a function of electron-impact energy. The red line refers to the full rovibrational frame transformation calculation. The black line give the ANR cross section while triangles denote the MQDT-RFT cross section. Vertical arrows denote the (1, 1) → (2, 1) and (1, 1) → (3, 1) thresholds.

over the Rydberg series and it provides, as expected, a good averaged description of the full MQDT rovibrational result. We also notice that despite a large effect of resonances on the excitation probabilities for $J_{\rm tot} = 2$ (a factor of 2, see Fig. 1), the resulting effect on the cross sections summed over $J_{\rm tot}$ is significantly lower, with an enhancement of about 30 %. This of course was expected since the dominant contribution to the cross section arises from a symmetry (here $J_{\rm tot} = 1$) with no purely rotational Rydberg series.

Below the energy of the lowest ionization channel, the excitation cross section in any MQDT treatment is identically zero, or strictly speaking, the cross-section is not defined there because the electron cannot be at infinity when all channels are closed. This behavior of the cross-section agrees with Wigner's laws (Wigner 1948, Stabler 1963).

It is important to note that the ANR excitation cross section follows the correct threshold law for an inelastic electron collision with a positive ion:

$$\lim_{E'_k \to 0} \sigma^{\rm ANR}_{JK\to J'K'}(E_k) \propto \frac{1}{E_k} = \text{non-zero constant} \tag{23}$$

This actually reflects the weak energy dependence of the ANR T-matrix elements, in agreement with the MQDT-RFT results (see section 2.2). As explained in section 2.1, however, the ANR cross sections are actually non-zero below threshold owing to our definition of the ANR energy. In Figs. 2 and 3, cross sections were therefore multiplied

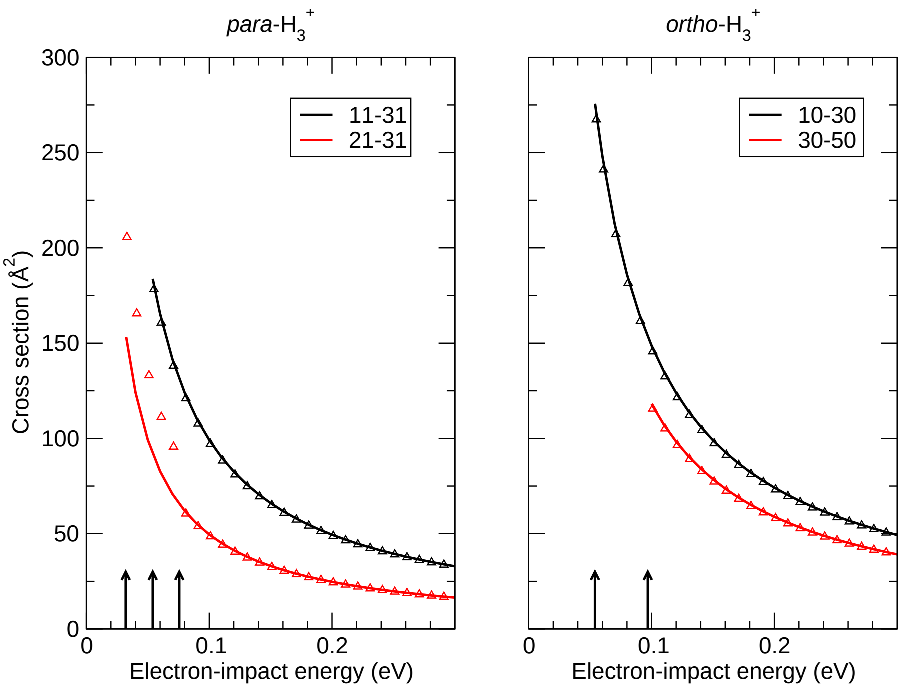

Figure 3. Rotationally inelastic cross section for four different transitions in H_3^+ as a function of electron-impact energy. Lines give ANR cross sections while triangles denote MQDT-RFT cross sections. Vertical arrows denote the involved thresholds.

by the following Heaviside step function :

$$H(E_k) = \begin{cases} 1 & \text{if } E_k \geq E_{th} \\ 0 & \text{if } E_k < E_{th}, \end{cases} \tag{24}$$

where $E_{th} = E_{J'K'} - E_{JK}$ is the threshold energy. This ad-hoc correction is the simplest way of forcing the cross section to zero below threshold while keeping a finite value at threshold, in agreement with the above theoretical considerations. The effect of this 'Heaviside correction' can be checked carefully in transitions with no rotational Rydberg series, that is, those with $\Delta J > 1$. In Fig. 3, we can thus observe that all ANR cross sections for transitions with $\Delta J = 2$ are in excellent agreement with those obtained at the MQDT-RFT level down to threshold. Of course, the exception is the $(2,1) \rightarrow (3,1)$ transition in which closed-channels effects occur at energies between the (3, 1) and (4, 1) channels and are of similar magnitude as in $(1,1) \rightarrow (2,1)$. Note that we actually observe a slight increase of closed channel effects as the initial J increases. Rydberg resonances were thus found to enhance the $(4,1) \rightarrow (5,1)$ cross section by about 45 % at energies between the (5, 1) and (6, 1) channels.

The results presented in Figs. 2 and 3 show that despite the important contribution of closed-channel effects in transitions with $\Delta J = 1$, the ANR theory is generally quite successful in predicting rotational cross sections for molecular ions down to threshold. This result was actually predicted by Chang and Temkin (1970), although the role of closed-channels was not considered by these authors. In their study, Chang and Temkin

(1970) showed that the correction term to the adiabatic equation (Eq. 2.1 of their paper) is of the order of the ratio of the electron mass m to that of the nuclei M. They concluded that the ANR theory should be accurate down to an energy:

$$E_k \gg (m/M)E_{th}, \tag{25}$$

that is, very close to threshold. It is interesting to notice that the same authors estimated that the lower limit in the case of neutral target molecules is much larger and is given by $E_k \geq 1.65E_{th}$. This huge difference reflects the influence of the strong Coulomb field in the case of ions.

We finally note that the above Heaviside correction does not of course correct for the breakdown of detailed balance within ANR theory. As discussed in section 2.3, a possible method to enforce detailed balance is to use a different definition of the ANR energy for excitation and deexcitation processes. However, as the present ANR T-matrix elements are nearly energy independent, detailed balance is actually almost satisfied at the ANR level. For practical applications such as rate coefficient calculations, we still recommend computing cross sections and rates for the excitation processes (including the Heaviside correction) and using the detailed balance relation for the reverse ones.

4. Conclusions

Near-threshold rotational excitation of H_3^+ by electron-impact has been investigated by comparing ANR cross sections with calculations based on the MQDT rotational-frame-transformation (MQDT-RFT) method (Kokoouline and Greene 2003). Very good agreement between ANR and MQDT-RFT cross sections is obtained for kinetic energies above the resonance regime caused by rotational closed-channels. These resonances occur for transitions with $\Delta J = 1$ and $\Delta K = 0$ and for these, an analytical formula for averaging transition probabilities over the resonance structure has been formulated. This averaging procedure is shown to significantly enhance probabilities and, to a lesser extent, cross sections. In the case of transitions with $\Delta J > 1$, the ANR theory is shown to be accurate down to threshold, provided a simple 'Heaviside correction' is applied to the excitation cross sections. An alternative but strictly equivalent solution is to interpret the ANR energy as the exit kinetic electron energy and to compute deexcitation cross sections.

Some previous studies of the rotational excitation of molecular ions by electron collision, such as the H_3^+ study by Faure and Tennyson (2002b), applied the "correction" factor k'/k, designed for neutral targets by Morrison (1988), in a manner that is not strictly correct. The resulting error in those results will be generally modest, nevertheless, except at energies very close to rotational thresholds. Ideally, those results should be revised along the lines implied by the more detailed analysis of the present study, including the average effects of closed channel resonances where appropriate. But this is beyond the scope of the present article, so we do not present a comprehensive set of revised excitation rate coefficients here. Moreover, the scattering matrices obtained in R-matrix calculations can be used even below closed-channel thresholds, provided they are

sufficiently smooth functions of energy, and provided they are used in combination with MQDT closed-channel elimination formulas. The excellent agreement between R-matrix ANR cross sections and the MQDT-RFT results in Figs. 2 and 3 provides supporting evidence for this point. This is also supported by the quantum defects as deduced from the R-matrix calculations (using the diagonal BF T-matrix elements restricted to the p-wave channels): we obtain μ_0=0.05 and $\mu_{\pm1}$=0.37, in very good agreement with the MQDT-RFT values of, respectively, 0.05 and 0.39 (see section 2.2.1).

The range of validity of the adiabatic theory is therefore much wider than the usual classically derived condition that the impacting electron energy be large compared to the threshold energy. Moreover, it should be stressed that H_3^+ is quite an unfavorable system for the ANR theory owing to its large rotational spacings that make threshold and closed-channel effects important up to large kinetic energies ($>$ 0.01 eV). In particular, for astrophysical applications where inelastic rate coefficients are required down to $\sim$10$-$100 K (Faure *et al* 2006), Rydberg resonances will play a significant role. In contrast, for ions with rotational spacings smaller than typically 10 K, resonances will be of minor importance. Finally, in the case of strongly polar ions ($\mu \gtrsim$2 D) such as HCO^+, rotational excitation is completely dominated by (dipolar) transitions with $\Delta J = 1$ (see, e.g. Faure and Tennyson (2001)). In this case, resonances due to the low probability transitions $\Delta J > 1$ should not contribute significantly to the dipolar cross sections. High-partial waves ($l > 1$) are, however, required to converge dipolar cross sections (i.e., the use of BF T-matrix elements actually leads to a divergent cross section). It will be thus important to investigate in future works the influence of closed-channels on d-, f- and higher partial wave contributions to the cross section.

Acknowledgments

This work has been supported by the National Science Foundation under Grant No. PHY-0427460 and Grant No. PHY-0427376, by an allocation of NERSC supercomputing resources. AF acknowledges support by the CNRS national program "Physique et Chimie du Milieu Interstellaire".

5. References

Aymar M, Greene C H, Luc-Koenig E 1996 *Rev. Mod. Phys.* **68** 1015
Bordas M C, Lembo L J and Helm H 1991 *Phys. Rev. A* **44** 1817
Chang E S and Fano U 1972 *Phys. Rev. A* **6** 173
Chang E S and Temkin A 1970 *J. Phys. Soc. Jpn.* **29** 172
Chase D M 1956 *Phys. Rev.* **104** 838
Chase D M 1957 *Phys. Rev.* **106** 516
Child M S and Jungen Ch 1990 *J. Chem. Phys.* **93** 7756
Chu S I and Dalgarno A 1974 *Phys. Rev. A* **10** 788
Chu S I 1975 *Phys. Rev. A* **12** 396
Dickinson A S and Muñoz J M 1977 *J. Phys. B: Atom. Molec. Phys.*
Fano U 1970 *Phys. Rev. A* **2** 353

Faure A and Tennyson J 2001 *Mon. Not. R. Astron. Soc.* **325** 443

Faure A, Gorfinkiel J D, Morgan L A and Tennyson J 2001 *Comput. Phys. Commun.* **144** 224

Faure A and Tennyson J 2002 *J. Phys. B.: At. Mol. Opt. Phys.* **35** 1865

Faure A and Tennyson J 2002 *J. Phys. B.: At. Mol. Opt. Phys.* **35** 3945

Faure A, Wiesenfeld L, Valiron P, Tennyson J 2006 *Phil. Trans. London Roy. Soc.* in press

Gao H and Greene C H 1990, *Phys. Rev. A* **42** 6946

Gianturco F A and Jain A 1986 *Phys. Rep.* **143** 347

Greene C H and Jungen Ch 1985 *Adv. At. Mol. Phys.* **21** 51

Hamilton E L and Greene C H 2002, *Phys. Rev. Lett.* **89** 263003

Kokoouline V and Greene C H 2003 *Phys. Rev. A* **68** 012703

Kokoouline V and Greene C H 2004 *Phys. Rev. A* **69** 032711

Lammich L *et al* 2003, *Phys. Rev. Lett.* **91** 143201

Lane N F 1980 *Rev. Mod. Phys.* **52** 29

Lim A J, Rabadán I and Tennyson J 1999, *Mon. Not. Roy. Astron. Soc.* **306** 473

Morrison M A 1988, *Adv. At. Mol. Phys.* **24** 51

Neufeld D A and Dalgarno A 1990 *Phys. Rev. A* **40** 633

Rabadán I, Sarpal B. K. and Tennyson J 1998, *J. Phys. B.: At. Mol. Opt. Phys.* **31** 2077

Stabler R C 1963, *Phys. Rev.* **131** 679

Stephens J A 1995, *J. Chem. Phys.* **102** 1579

Wigner E P 1948 *Phys. Rev.* **73** 1002